



MODELLING OF PROCESSES OF HEAT-, MASS- AND ELECTRIC TRANSFER IN COLUMN AND ANODE REGION OF ARC WITH REFRACTORY CATHODE

I.V. KRIKENT¹, I.V. KRIVTSUN² and V.F. DEMCHENKO²

¹Dneprodzerzhinsk State Technical University, Dneprodzerzhinsk, Ukraine

²E.O. Paton Electric Welding Institute, NASU, Kiev, Ukraine

Numerical analysis of thermal, electromagnetic and gas-dynamic characteristics of plasma of free-burning arc in argon at atmospheric pressure with tungsten cathode and copper water-cooled anode was performed in the anode region and column of welding arc based on self-consistent mathematic model of processes of heat-, mass- and electric transfer. Results of calculation of current density on the anode and heat flow in the anode are compared with the available experimental data. It is shown that considering of the anode potential drop in the model provides more accurate predictions of the characteristics of heat and electric interaction of arc plasma with anode surface.

Keywords: fusion welding, electric arc, refractory cathode, arc characteristics, modelling of heat-, mass- and electric transfer

Information about thermal, electric and dynamic effects of arc on welded metal is necessary for efficient application of the electric arc as a heat source in fusion welding. Investigation of welding arcs using the mathematic modelling methods [1–8] seems to be relevant since experimental determination of characteristics of the welding arc important from technological point of view such as density of electric current and heat flow over the surface of welded part is complicated due to high values of temperature of arc plasma and metal surface temperature, small geometry of region of arc fixation and series of other factors.

Let us consider the electric arc with refractory cathode burning in inert gas at atmospheric pressure. The main attention will be given to the processes taking place in a column and anode region of the arc since theory and mathematic models of cathode phenomena, including processes in a near-cathode plasma, were developed in sufficient details for such an arc [9–12]. Study [13] proposed a self-consistent mathematic model of indicated processes for conditions of nonconsumable electrode welding and plasma welding. The aim of the present work is a verification of given model by means of numerical investigation of distributed characteristics of plasma of column and anode region of a free-burning arc with tungsten cathode and copper water-cooled anode and comparison of obtained results with available experimental data.

Two interconnected models are included in the self-consistent mathematic model of the processes of energy-, mass- and electric transfer in the column and anode region of the welding arc with refractory cathode in accordance with approach applied in [13]:

- model of arc column describing interaction of thermal, electromagnetic, gas-dynamic and diffusion processes in multicomponent plasma of the arc column;
- model of anode region which allows determining characteristics of thermal and electric interaction of arc with anode surface (part), necessary for analysis of thermal, electromagnetic and hydro-dynamic processes in welded metal.

Model of the anode region of arc with evaporating anode proposed in study [13] allows calculating distribution of anode potential drop $U_a = -\Delta\phi$ along the anode surface and density of heat flow q_a , being entered in the anode by arc, depending on current density on the anode j_a , temperature of electrons of plasma near the anode T_{ea} as well as temperature of its surface T_s . Distribution of j_a and T_{ea} along the anode surface can be determined with sufficient accuracy in modelling of the arc with refractory cathode based on the model of arc column with self-consistent boundary conditions on the anode.

Comparison of calculation value $\Delta\phi$ with one experimentally measured for the case of application of the arc with tungsten cathode and copper water-cooled anode burning in argon at atmospheric pressure (arc current 200 A, 10 mm length) was carried out for verification of conformity of selected model of anode processes. The following experimental data [14, 15] were used in calculations: $j_a = 3.5 \cdot 10^6$ A/m², $T_{ea} = 9840$ K, $T_s = 720$ K, that provides $\Delta\phi = 4.04$ V. Obtained calculation value complies with experimentally measured $\Delta\phi = 4.01$ V [15] with high accuracy. Figures 1 and 2 show applied in further calculation dependencies of $\Delta\phi$ and q_a on temperature of electrons in the near-anode plasma and density of electric current on the anode for the free-burning argon arc with refractory cathode and copper water-cooled anode.



Model of isothermal plasma (temperature of electrons equals temperature of heavy particles) was used in describing the processes of heat-, mass- and electric transfer in column plasma of the considered arc, and distribution of all its characteristics as axial-symmetric would be considered. The corresponding system of differential equations represented in a cylindrical coordinate system $\{r, \vartheta, z\}$ has the following appearance [13]:

- continuity equation

$$\frac{\partial \rho}{\partial t} + \frac{1}{r} \frac{\partial}{\partial r} (r\rho v) + \frac{\partial}{\partial z} (\rho u) = 0, \quad (1)$$

where ρ is the mass density of plasma; v, u are the radial and axial components of its speed;

- motion equations

$$\begin{aligned} \rho \left(\frac{\partial v}{\partial t} + v \frac{\partial v}{\partial r} + u \frac{\partial v}{\partial z} \right) = & - \frac{\partial p}{\partial r} - j_z B_\varphi + \frac{2}{r} \frac{\partial}{\partial r} \times \\ & \times \left(r\eta \frac{\partial v}{\partial r} \right) + \frac{\partial}{\partial z} \left[\eta \left(\frac{\partial u}{\partial r} + \frac{\partial v}{\partial z} \right) \right] - \\ & - 2\eta \frac{v}{r^2} - \frac{2}{3} \frac{\partial}{\partial r} \left\{ \eta \left[\frac{1}{r} \frac{\partial(rv)}{\partial r} + \frac{\partial u}{\partial z} \right] \right\}, \end{aligned} \quad (2)$$

$$\begin{aligned} \rho \left(\frac{\partial u}{\partial t} + v \frac{\partial u}{\partial r} + u \frac{\partial u}{\partial z} \right) = & - \frac{\partial p}{\partial z} + j_r B_\varphi + 2 \frac{\partial}{\partial z} \times \\ & \times \left(\eta \frac{\partial u}{\partial z} \right) + \frac{1}{r} \frac{\partial}{\partial r} \left[r\eta \left(\frac{\partial u}{\partial r} + \frac{\partial v}{\partial z} \right) \right] - \\ & - \frac{2}{3} \frac{\partial}{\partial z} \left\{ \eta \left[\frac{1}{r} \frac{\partial(rv)}{\partial r} + \frac{\partial u}{\partial z} \right] \right\}, \end{aligned} \quad (3)$$

where p is the pressure; j_z, j_r are the axial and radial components of current density in the arc; B_φ is the azimuth component of vector of magnetic induction; η is the coefficient of dynamic viscosity;

- energy equation

$$\begin{aligned} \rho C_p \left(\frac{\partial T_p}{\partial t} + v \frac{\partial T_p}{\partial r} + u \frac{\partial T_p}{\partial z} \right) = & \frac{1}{r} \frac{\partial}{\partial r} \times \\ & \times \left(r\chi \frac{\partial T_p}{\partial r} \right) + \frac{\partial}{\partial z} \left(\chi \frac{\partial T_p}{\partial z} \right) + \frac{k}{e} \times \\ & \times \left\{ j_r \frac{\delta[(5/2 - \delta)T_p]}{\partial r} + j_z \frac{\delta[(5/2 - \delta)T_p]}{\partial z} \right\} + \\ & + \frac{j_r^2 + j_z^2}{\sigma} - \psi, \end{aligned} \quad (4)$$

where C_p is the specific heat capacity of plasma considering ionization energy; T_p is the plasma temperature; χ is the coefficient of heat conductance; k is the Boltzmann constant; e is the charge of electron; δ is the thermodiffusion constant; ψ is the energy loss for radiation in approximation of optically thin plasma;

- equations of electromagnetic field

$$\frac{1}{r} \frac{\partial}{\partial r} \left(r\sigma \frac{\partial \varphi}{\partial r} \right) + \frac{\partial}{\partial z} \left(\sigma \frac{\partial \varphi}{\partial z} \right) = 0, \quad (5)$$

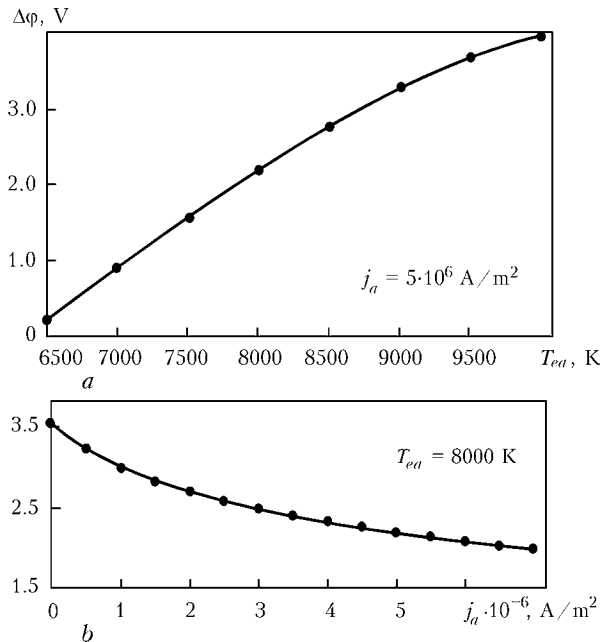


Figure 1. Dependence of potential differences between the boundary of arc column and anode surface on temperature of electrons in the anode region (a) and density of electric current on the anode (b) for argon arc with copper water-cooled anode

$$B_\varphi(r, z) = \frac{\mu^0}{r} \int_0^r j_z(\xi, z) \xi d\xi, \quad (6)$$

where φ is the electric potential; σ is the plasma specific electric conductivity; μ^0 is the universal magnetic constant;

$$j_r = -\sigma \frac{\partial \varphi}{\partial r}, \quad j_z = -\sigma \frac{\partial \varphi}{\partial z}. \quad (7)$$

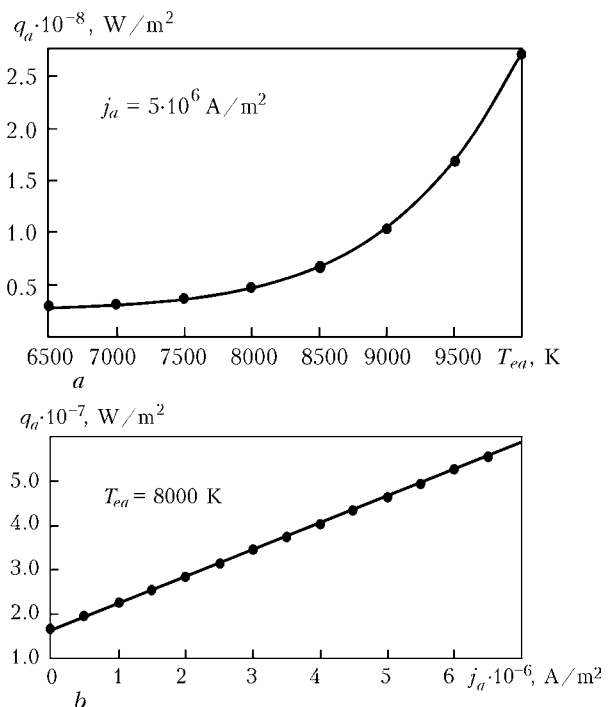


Figure 2. Dependence of heat flow in the anode on temperature of electrons in the anode region (a) and density of electric current on the anode (b) for argon arc with copper water-cooled anode



Thermodynamic characteristics ρ , C_p , coefficients of transfer η , χ , δ , σ and loss of energy for irradiation ψ of arc plasma depending on its temperature, pressure and composition are to be put for closing the system of equations (1)–(7). Study [16], for example, provides indicated dependencies for isothermal argon plasma of atmospheric pressure.

Corresponding initial and boundary conditions are to be set for solving the system of differential equations (1)–(5) describing the processes of heat-, mass- and electric transfer in the arc column. Initial distributions of speed and temperature of plasma have no fundamental importance since physical fields are established sufficiently quickly in the arc discharge. For example, zero values can be set for speed, and temperature in the region of current channel can be chosen such as to provide plasma conductivity character for the argon arc.

Boundary conditions for desired functions ($\nabla = \{v, 0, u\}$, T_p , φ) were formulated in the following way for case of considered here arc with tungsten cathode and copper water-cooled anode.

«Adhesion» conditions are fulfilled for plasma speed ∇ on the surface of anode (plane $z = L$):

$$\nabla|_{z=L} = 0. \quad (8)$$

The following condition of energy balance [13] takes place on the boundary of plasma of the arc column with the anode region:

$$-\chi \frac{\partial T_p}{\partial z}|_{z=L} + j_a \frac{k}{e} \left(\frac{5}{2} - \delta \right) T_p|_{z=L} = \Delta\varphi j_a + q_a, \quad (9)$$

where $j_a = -j_z|_{z=L}$ is the current density on the anode.

Electric potential of the anode surface can be considered constant and equal zero at good approximation. Then the boundary condition for potential on the boundary of arc column with the anode region can be written as

$$\varphi|_{z=L} = \Delta\varphi. \quad (10)$$

Potential drop $\Delta\varphi$ in expressions (9), (10) is calculated according to the model of the anode region [13] at $T_{ea} = T_p|_{z=L}$ (see Figure 1).

The conditions for vector of speed near the cathode (plane $z = 0$) are set in the following way:

$$v|_{z=0} = 0, \quad u|_{z=0} = u_0, \quad (11)$$

where u_0 is determined by consumption of shielding gas and diameter of nozzle for its feeding.

We will take the following conditions for temperature and electric potential in the near cathode zone of arc:

$$T_p|_{z=0} = T_k(r), \quad \sigma \frac{\partial \varphi}{\partial z}|_{z=0} = j_k(r), \quad (12)$$

where distribution of plasma temperature $T_k(r)$ and current density under the cathode $j_k(r)$ are chosen according to the recommendations of study [12].

It can be indicated in the zone of shielding gas supply that

$$T_p|_{z=0} = T_{env}, \quad \frac{\partial \varphi}{\partial z}|_{z=0} = 0, \quad (13)$$

where T_{env} is the temperature of environment.

The boundary conditions for speed, temperature of plasma and electric potential on the axis of symmetry of the system are set in the standard way (see, for example, [1, 3]).

We can write [3] on the outer boundary of calculation area ($r = R$) for speed of plasma and electric potential

$$\frac{\partial(\rho v r)}{\partial r}|_{r=R} = 0, \quad u|_{r=R} = 0, \quad \frac{\partial \varphi}{\partial r}|_{r=R} = 0. \quad (14)$$

The boundary condition for temperature of plasma at $r = R$ will be determined depending on moving direction of the plasma flow:

$$T_p|_{r=R} = T_{env} \text{ at } v|_{r=R} \leq 0, \quad (15)$$

$$\frac{\partial T_p}{\partial r}|_{r=R} = 0 \text{ at } v|_{r=R} > 0.$$

A finite-difference method was used for numerical solving of the system of differential equations (1)–(5) with the boundary conditions (8)–(15). Calculation data for argon plasma [16] were used for determination of the thermodynamic and transport characteristics of plasma included in equations (1)–(5). Common Lagrangian–Eulerian method [17, 18] adapted to the conditions of compressible media was used at numerical solution of the gas-dynamic and thermal tasks.

A zone φ of positive values, caused by the presence of reverse potential drop on the anode layer, appears over the surface of anode, as can be seen from results of calculation of the electric potential (Figure 3, *a*). The maximum values of gradient of potential and current density in the arc column can be observed near the cathode (Figure 3, *b*). The maximum temperature of arc plasma (Figure 4, *a*) is also achieved in this place that is caused by high intensity of Joule heat sources. Density of electric current rapidly reduces (see Figure 3, *b*) as the distance from the cathode increases. Pattern of plasma movement in the arc column (see Figure 4, *b*) character for the arc with refractory cathode is caused by a force field formed at such current distribution. The maximum values of plasma speed on the axis of symmetry (up to 350 m/s) provide efficient transfer of heat energy from the hottest zone near the cathode to the anode surface. As can be seen from Figure 4, *a*, convective heat transfer determines the temperature field in the arc plasma to a substantive level. This fact explains significant elongation of isotherms along the anode surface.

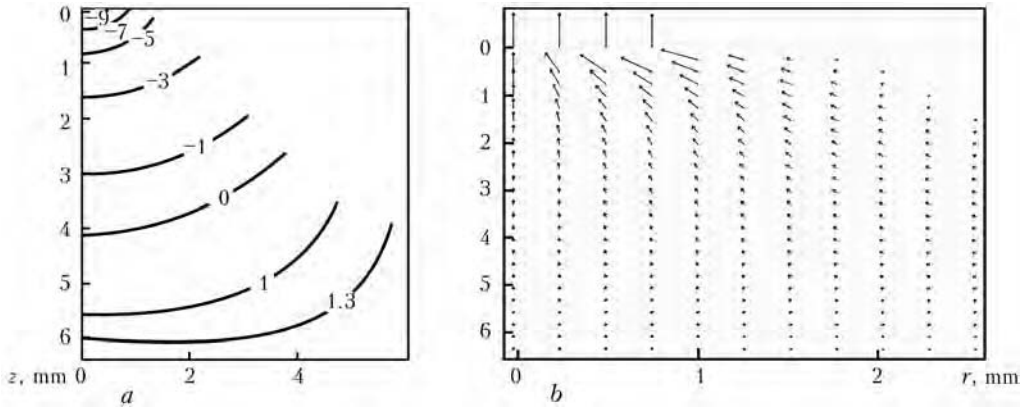


Figure 3. Fields of electric potential (a) and current density (b) in the column of free-burning arc in argon with tungsten cathode and copper water-cooled anode ($\max |\vec{j}| = 8 \cdot 10^7 \text{ A/m}^2$)

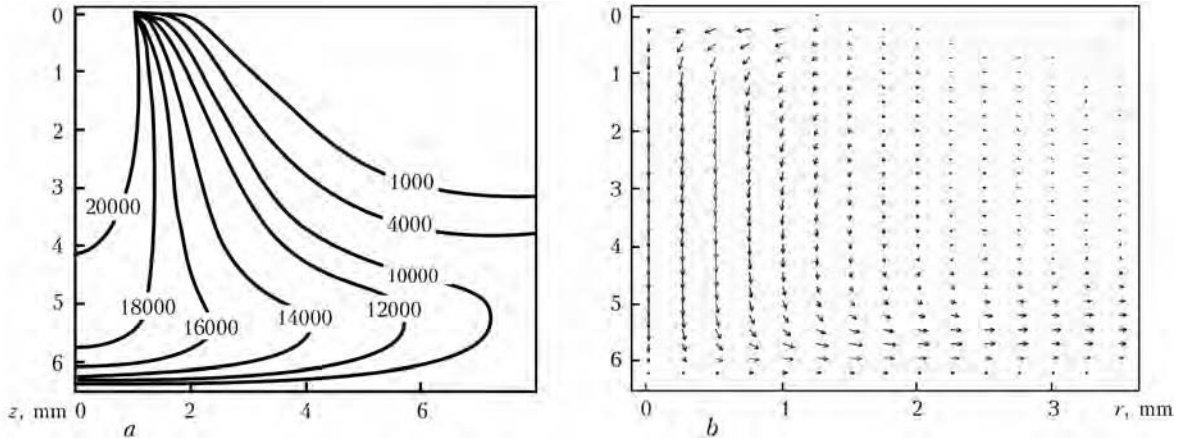


Figure 4. Fields of temperature (a) and speed (b) of plasma in the column of free-burning arc in argon with tungsten cathode and copper water-cooled anode ($\max |\vec{V}| = 8 \cdot 10^7 = 350 \text{ m/s}$)

Figure 5 shows that the maximum value of $\Delta\phi$ in the near-anode region is caused by higher values of T_{ea} near the axis of symmetry. Certain increase of the potential drop on a periphery of region of anode arc fixation is caused by extremely small value of current density in this region of the anode surface.

Figure 6 shows a comparison of calculation data of radial distribution of electric current density on the anode and heat flow in the anode with experimental ones [14]. Sufficiently good matching of calculation distributions $j_a(r)$ and $q_a(r)$ with experimental ones is observed for arc of 200 A current. Some differences in calculation and experimental data near the axis of symmetry can be related with the errors of mathematic

modelling as well as with the problems of reconstruction of distributed characteristics on integral parameters, measured in [14]. Compliance of the results of mathematic modelling and experimental data for arc of 100 A can be described as sufficiently satisfactory.

The numerical analysis of distributed characteristics in the column and anode region of the electric arc with tungsten cathode and copper water-cooled

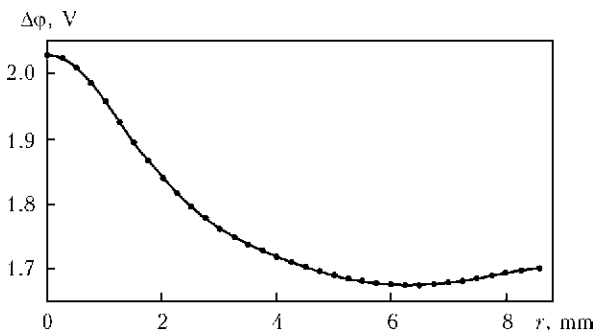


Figure 5. Radial distribution of potential drop in the anode region for free-burning arc in argon with tungsten cathode and copper water-cooled anode ($I = 200 \text{ A}$, $L = 6.3 \text{ mm}$, $T_s = 720 \text{ K}$)

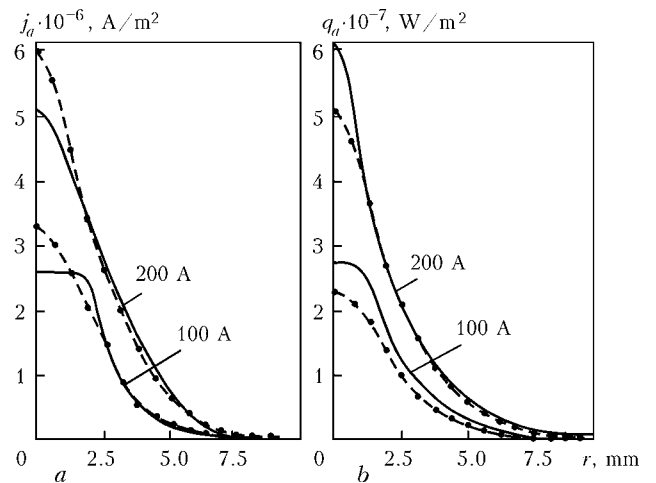


Figure 6. Radial distributions of current density on the anode (a) and heat flow in the anode (b) for free-burning arc in argon with tungsten cathode and copper water-cooled anode ($L = 6.3 \text{ mm}$) [14]: dashed curves — calculation; solid — experimental data



anode and comparison of obtained results with available experimental data performed in this study on the whole are an evidence of adequacy of the self-consistent model proposed in study [13] for processes of heat-, mass- and electric transfer in the anode region and column of welding arc in nonconsumable electrode welding and plasma welding in inert gas.

1. Hsu, K.C., Etemadi, K., Pfender, E. (1983) Study of the free-burning high-intensity argon arc. *J. Appl. Phys.*, 54(3), 1293–1301.
2. Hsu, K.C., Pfender, E. (1983) Two-temperature modeling of the free-burning high-intensity arc. *Ibid.*, 54(8), 4359–4366.
3. Zhu, P., Lowke, J.J., Morrow, R. et al. (1995) Prediction of anode temperatures of free burning arcs. *J. Phys. D: Appl. Phys.*, 28, 1369–1376.
4. Lowke, J.J., Morrow, R., Haidar, J. (1997) A simplified unified theory of arcs and their electrodes. *Ibid.*, 30, 2033–2042.
5. Haidar, J. (1999) Non-equilibrium modeling of transferred arcs. *Ibid.*, 32, 263–272.
6. Fan, H.G., Kovacevic, R. (2004) A unified model of transport phenomena in gas metal arc welding including electrode, arc plasma and molten pool. *Ibid.*, 37, 2531–2544.
7. Hu, J., Tsai, H.L. (2007) Heat and mass transfer in gas metal arc welding. Pt 1: The arc. *Int. J. Heat and Mass Transfer*, 50, 833–846.
8. Tanaka, M., Yamamoto, K., Tashiro, S. et al. (2008) Metal vapour behaviour in gas tungsten arc thermal plasma during welding. *Welding in the World*, 52(11/12), 82–88.
9. Mojzhes, B.Ya., Nemchinsky, V.A. (1972) To theory of high pressure arc on refractory cathode. *Zhurnal Tekhnich. Fiziki*, 42(5), 1001–1009.
10. Mojzhes, B.Ya., Nemchinsky, V.A. (1973) To theory of high pressure arc on refractory cathode. Pt 2. *Ibid.*, 43(11), 2309–2317.
11. Zhukov, M.F., Kozlov, N.P., Pustogarov, A.V. et al. (1982) *Near-electrode processes in arc discharges*. Novosibirsk: Nauka.
12. Wendelstorf, J., Simon, G., Decker, I. et al. (1997) Investigation of cathode spot behaviour of atmospheric argon arcs by mathematical modeling. In: *Proc. of 12th Int. Conf. on Gas Discharges and Their Applications* (Germany, Greifswald, 1997), Vol. 1, 62–65.
13. Krivtsov, I.V., Demchenko, V.F., Krikent, I.V. (2010) Model of the processes of heat, mass and charge transfer in the anode region and column of the welding arc with refractory cathode. *The Paton Welding J.*, 6, 2–9.
14. Nestor, O.H. (1962) Heat intensity and current density distributions at the anode of high current, inert gas arcs. *J. Appl. Phys.*, 33(5), 1638–1648.
15. Sanders, N.A., Pfender, E. (1984) Measurement of anode falls and anode heat transfer in atmospheric pressure high intensity arcs. *Ibid.*, 55(3), 714–722.
16. Boulos, M.I., Fauchais, P., Pfender, E. (1997) *Thermal plasmas: Fundamentals and applications*. Vol. 1. New-York; London: Plenum Press.
17. Lyashko, I.I., Demchenko, V.F., Vakulenko, S.A. (1981) Version of dynamics equation splitting method of viscous incompressible fluid on Lagrangian-Eulerian networks. *Doklady AN UkrSSR, Series A*, 43–47.
18. Demchenko, V.F., Lesnoj, A.B. (2000) Lagrangian-Eulerian method for numerical solution of multidimensional problems of convective diffusion. *Dopovidi NAN Ukrainy*, 11, 71–75.

EFFICIENCY OF ELECTRODYNAMIC TREATMENT OF WELDED JOINTS OF AMg6 ALLOY OF DIFFERENT THICKNESS

L.M. LOBANOV, N.A. PASHCHIN and O.L. MIKHODUJ
E.O. Paton Electric Welding Institute, NASU, Kiev, Ukraine

Influence of design features of fastening the samples of AMg6 alloy and its welded joints in the grips of testing machine on decrease in deformation resistance at electrodynamic treatment is shown. It is established that the effectiveness of electrodynamic effect is decreased with increase in thickness of metal being treated.

Keywords: welded joints, aluminium alloy, electrodynamic treatment, initial stresses, current discharge, charge voltage, system of specimen fastening, efficiency of treatment, decrease of deformation resistance

The methods of treatment of metallic materials by pulse electromagnetic fields are ever more widely used in control of stressed state of elements of welded structures [1, 2]. One of the methods of pulse effect by electric current on metals and alloys is electrodynamic treatment (EDT). The investigations of mechanisms of influence of EDT on stressed state of aluminium alloys [3], structural steels [4, 5] and also welded joints of these materials were conducted. The results presented in the works [1, 3–5] were obtained using developed experimental methods based on tension of flat specimens, their treatment by current discharges with in-process control of change in tension force which was taken as evaluation characteristics of EDT.

At the same time it is known [6] that conditions of fastening of specimens being investigated in the grips of testing machine have considerably greater influence on resistance of metallic materials to deformation at dynamic loads than at static ones. The same concerns the deformation processes initiated in the metals and alloys by passing of charges of electric current [7].

Thus, it is obvious that during evaluation of EDT process efficiency it is necessary to consider the design system of fastening the specimens being treated. Moreover, basing on the analysis of fractograms of fractures of AMg6 alloy it is assumed that the efficiency of electrodynamic effect is decreased with increase in thickness of metal being treated [8]. The quantitative evaluation of EDT efficiency depending on thickness of treated material allows distinguishing the range of values of power parameters of electrodynamic effect defining the applicability of this method of treatment in the engineering practice.